Towards unified description of hot nuclei fission

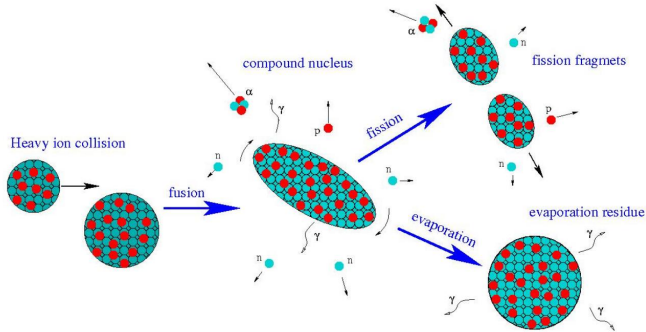

Krzysztof Pomorski

Department of Theoretical Physics, MCS University, Lublin, Poland

SSNET-20, 4th - 8th November, Orsay, France

Results presented here* are obtained in collaboration with

- UMCS - Lublin:
  B. Nerlo-Pomorska
- IPHC DRS - Strasbourg:
  J. Bartel, C. Schmitt
- TU - Beijing:
  Z.G. Xiao
- CIAE NDC - Beijing:
  Y.J. Chen, L.L. Liu

Our research was supported by the Natural Science Foundation of China, (Grant No. 11961131010 and 12275081) and by the Polish-French agreement COPIN-IN2P3, project No. 08-131 and 15-149.

* K. Pomorski, B. Nerlo-Pomorska, J. Bartel, C. Schmitt, Z. G. Xiao, Y. J. Chen, L. L. Liu, Phys. Rev. C 110, 034607 (2024).

Outline:

- Introduction
- Fourier over Spheroid (FoS) type parametrization of shapes of nuclei.
- Description of macroscopic-microscopic model.
- Potential energy surfaces of ^{250}Cf and ^{252}Cf within FoS parametrization.
- Dynamical evolution by Langevin and Master equations.
- Spontaneous fission yields of ^{252}Cf.
- Fission yields of ^{250}Cf at E^*=46 MeV.
- Summary

Introduction

Our 3D Langevin-plus-Masters model* applied to the thermal neutron induced fission of $^{236}\mathrm{U_{th}}^{*}$ has given the following mass, charge, TKE, and neutron multiplicity yields:

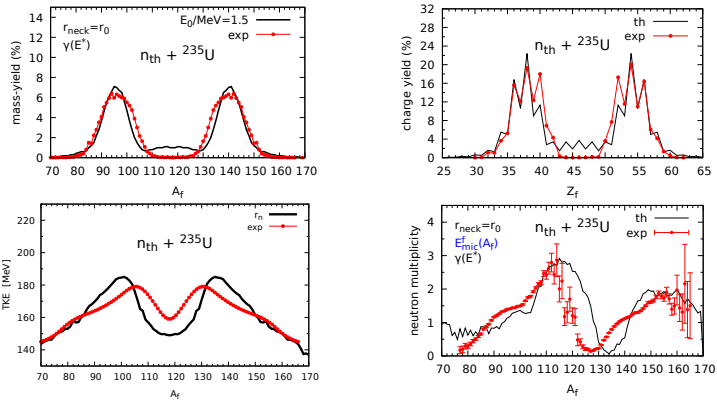

So, encouraged by the above results, we have applied this model, with the same parameter set, to describe the spontaneous fission of ^{252}Cf and heavy ion induced fission of ^{250}Cf.

* K. Pomorski, B. Nerlo-Pomorska, C. Schmitt, Z.G. Xiao, Y.J. Chen, L.L. Liu, PRC 107, 054616 (2023).

Fourier over Spheroid shape parametrization*

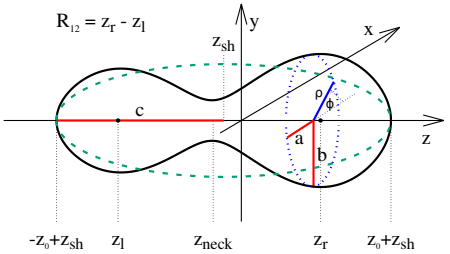

Non-axial shapes: $(x, y, x) \to (\rho, \varphi, z)$

$$\eta = \frac{b-a}{a+b}\,; \quad a(z)b(z) = \rho_s^2(z)$$

The parameter η is similar, but more general, than the γ-deformation of Åge Bohr.

The distance from the z-axis to the surface is given by:

$$\rho^2(z,\varphi) = \frac{R_0^2}{c}\, f\left(\frac{z - z_{\rm sh}}{z_0}\right) \frac{1-\eta^2}{1+\eta^2+2\eta\cos(2\varphi)}\,.$$

where

$$f(u) = 1 - u^2 - \sum_{k=1}^{n} \left\{ a_{2k}\cos\left(\tfrac{k-1}{2}\pi u\right) + a_{2k+1}\sin(k\pi u)\right\}\,,$$

Here $u = (z - z_{\rm sh})/z_0$ and $-1 \le u \le 1$, $z_0 = cR_0$ is the half-length of nucleus, R_0 is the radius of spherical nucleus, $z_{\rm sh} = -3/(4\pi)\, z_0(a_3 - a_5/2 + \ldots)$ is the shift to keep the mass-center at the coordinate origin, and a_i play a role of the deformation parameters.
The volume conservation is ensured by assuming $a_2 = a_4/3 - a_6/5 + \ldots$.

* K. Pomorski, B. Nerlo-Pomorska, Acta Phys. Pol. B Proc. Suppl. 16, 4-A021 (2023).

Potential energy surfaces of ^{252}Cf

The PES are evaluated within the macro-micro model using the LSD model and Yukawa-folded single-particle potential.

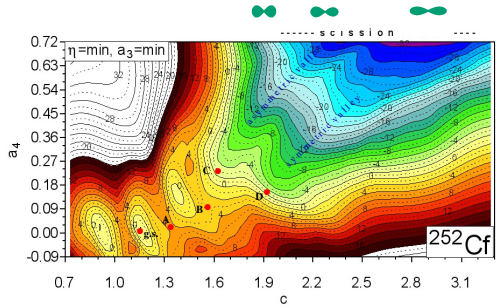

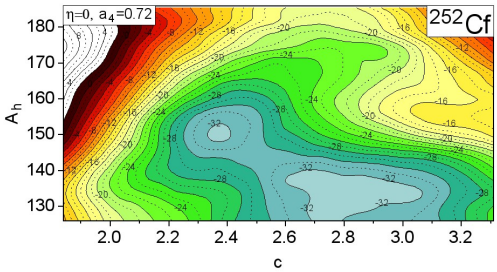

The values of the energy layers are taken relative to the spherical liquid drop binding energy.
Here, c is the elongation of nucleus, a_3 its left-right asymmetry, a_4 controls the neck size,
The geometric scission point appears when $a_4 = a_4^{sc} = \frac{3}{4} + \frac{6}{5}a_6 \ldots$ and $a_3 = 0$.
At the scission when $r_{neck} = r_n$ mass of the heavy fragment is $A_h \approx (1 + a_3)\frac{A}{2}$.

Temperature dependence of the microscopic energy

Due to energy-dissipation effects, even spontaneously fissioning nuclei get excited near the scission configuration. The temperature effect is even more crucial in the case of neutron-induced fission or the fission of compound nuclei formed in heavy-ion collisions.

In the macro-micro model, one assumes that the total potential energy:

$$E_{\rm pot}(def, T) = E_{\rm mac}(def, T) + E_{\rm mic}(def, T)$$

is the sum of the macroscopic and microscopic parts. The macroscopic energy $E_{\rm mac}$ grows parabolically with increasing temperature

$$E_{\rm mac}(def, T) = E_{\rm mac}(def, 0) + a(def)T^2$$

where a is the average single-particle level density*.
The microscopic energy $E_{\rm mic}$ decreases with temperature and we have assumed the following temperature dependence*:

$$E_{\rm mic}(def, T) \approx \frac{E_{\rm mic}(def, T = 0)}{1 + \exp((T - 1.5)/0.3)} ,$$

where T is in MeV units.

*B. Nerlo-Pomorska, K. Pomorski, J. Bartel, Phys. Rev. C 74, 034327 (2006).

Langevin dynamics

In our approach, the dissipative fission dynamics is described by the set of Langevin equations. In the generalized coordinates $(\{q_i\},\ \ i = 1, 2, ..., n)$ it has the following form:

$$\begin{aligned} \frac{dq_i}{dt} &= \sum_j [\mathcal{M}^{-1}(\vec{q})]_{ij}\, p_j \\ \frac{dp_i}{dt} &= -\frac{1}{2}\sum_{j,k} \frac{\partial [\mathcal{M}^{-1}]_{jk}}{\partial q_i}\, p_j\, p_k - \frac{\partial V(\vec{q})}{\partial q_i} \\ &\quad - \sum_{j,k} \gamma_{ij}(\vec{q})\, [\mathcal{M}^{-1}]_{jk}\, p_k + \mathcal{F}_i(t)\ , \end{aligned}$$

and

$$V(\vec{q}) = E_{\rm pot}(\vec{q}, 0) - a(\vec{q})\, T^2$$

is the Helmholtz free-energy of the fissioning nucleus with temperature T and $\vec{\mathcal{F}}$ is the Langevin random force.

The potential energy $E_{\rm pot}$ at a given deformation $\vec{q}$ is obtained by the macro-micro prescription. The inertia and friction tensors $\mathcal{M}_{jk}$ and γ_{ij} are evaluated in the irrotational flow and the wall approximation*.

*J. Bartel, B. Nerlo-Pomorska, K. Pomorski, A. Dobrowolski, Comp. Phys. Comm. 241, 139 (2019).

Fission fragment charge distribution*

Knowing the fission fragment deformations at scission $\vec{q}_l$ and $\vec{q}_{\rm h}$, it is possible to find the most probable charge for each isobar by analyzing the energy of the system at scission as a function of the charge number $Z_{\rm h}$ of the heavy fragment:

$$\begin{aligned} E(Z_{\rm h}; Z, A, A_{\rm h}, \vec{q}_{\rm h}, \vec{q}_l) &= E_{\rm LSD}(Z - Z_{\rm h}, A - A_{\rm h}); \vec{q}_l) \\ &+ E_{\rm LSD}(Z_{\rm h}, A_{\rm h}; \vec{q}_{\rm h}) + E^{\rm rep}_{\rm Coul} - E_{\rm LSD}(Z, A; 0) \ , \end{aligned}$$

where $A_{\rm h}$ is the heavy fragment mass number and the Coulomb repulsion energy $E^{\rm rep}_{\rm Coul}$ of the fragments is given by

$$\begin{aligned} E^{\rm rep}_{\rm Coul} &= \tfrac{3e^2}{5r_0} \left[\tfrac{Z^2}{A^{1/3}} B_{\rm Coul}(\vec{q}_{\rm sc}) \right. \\ &\left. - \tfrac{Z_{\rm h}^2}{A_{\rm h}^{1/3}} B_{\rm Coul}(\vec{q}_{\rm h}) - \tfrac{Z_l^2}{A_l^{1/3}} B_{\rm Coul}(\vec{q}_l) \right] . \end{aligned}$$

Here, $r_0 = 1.217$ fm is the charge radius constant and the Coulomb deformation dependent function, and $B_{\rm Coul}$ is the shape dependent coefficient the same as in the LSD mass formula.

* K. Pomorski, B. Nerlo-Pomorska, C. Schmitt, Z.G. Xiao, Y.J. Chen, L.L. Liu, PRC 107, 054616 (2023).

Shapes of the mother and the fragment nuclei at scission

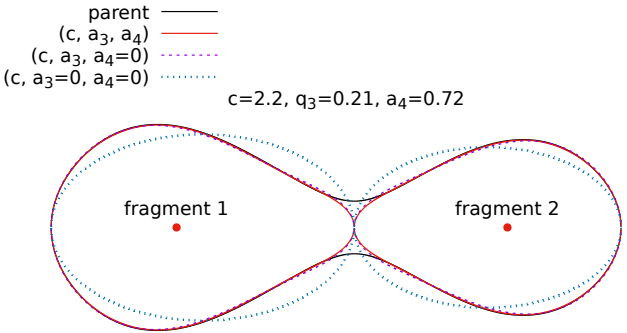

$c^{(1)}$=1.384, $a_3^{(1)}$=-0.361, $a_2^{(1)}$=-0.021; $c^{(2)}$=1.403, $a_3^{(2)}$= 0.312, $a_4^{(2)}$=-0.033

The fission fragments have frequently a pear-like shapes (red line). Omitting of this degree of freedom in some parametrizations (e.g. in the quadratic shapes of revolution parametrization) may lead to significant overestimation of the Coulomb repulsion energy of fragments.

On total energy and charge distribution probability

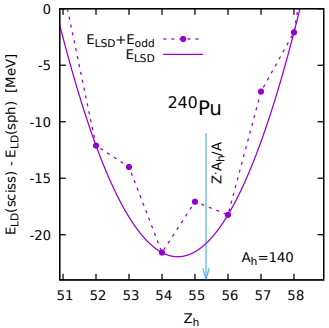

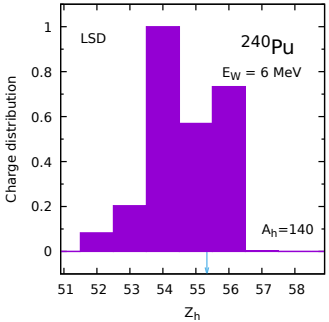

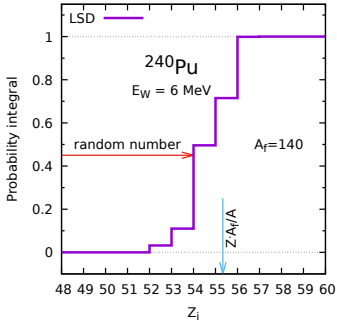

The Wigner function corresponding to the thermal excitation E^* of the fissioning nucleus at the scission point: $W(Z_i) = \exp[-(E_i - E_{min})^2/E_0^2]$ gives the distribution probability of the charge of the fragment. Here E_{min} is the lowest discrete energy as function of Z_i and a subsequent random number decides about the charge number Z_h of the heavy fragment, with $Z_l = Z - Z_h$. The parameter E_0 is taken here around the $\frac{1}{2}\hbar\omega_0$ value.

The above effect has to be taken into account at the end of each Langevin trajectory, when one fixes the (integer) fragment mass and charge numbers.

Kinetic energy of the fission fragments

Total kinetic energy (TKE) of the fragments $E_{\rm kin}^{\rm frag}$ is given by the sum of the Coulomb repulsion energy ($V_{\rm Coul}$), the nuclear interaction energy of fragments ($V_{\rm nuc}$), and the pre-fission kinetic energy of the relative motion ($E_{\rm kin}^{\rm coll}$) evaluated at the scission point ($q_{\rm sc}$):

$$E_{\rm kin}^{\rm frag} = V_{\rm Coul}(q_{\rm sc}) + V_{\rm nuc}(q_{\rm sc}) + E_{\rm kin}^{\rm coll}(q_{\rm sc}) \ .$$

The Coulomb repulsion energy is equal to the difference between the total Coulomb energy of the nucleus at the scission configuration and the Coulomb energies of the both deformed fragments:

$$V_{\rm Coul} = \frac{3e^2}{5r_0}\left[\frac{Z^2}{A^{1/3}}\,B_{\rm Coul}(q_{sc}) - \frac{Z_1^2}{A_1^{1/3}}\,B_{\rm Coul}(q_1) - \frac{Z_2^2}{A_2^{1/3}}\,B_{\rm Coul}(q_2)\right] \ .$$

It is a more accurate estimate of the Coulomb energy than the frequently used point-to-point (p-p) approximation: $E_{\rm kin}^{\rm pp} = e^2 Z_1 Z_2 / R_{12}$.

The nuclear interaction energy between the fragments at the scission point is approximately equal to the change of the nuclear surface energy when the neck breaks:

$$V_{\rm nuc}(q_{\rm sc}) = -2E_{\rm surf}^{\rm sph}\,\frac{\pi r_{\rm neck}^2({\rm sc})}{4\pi R_0^2} = -\frac{1}{2}E_{\rm surf}^{\rm sph}\left(\frac{r_{\rm neck}}{R_0}\right)^2$$

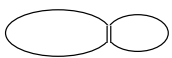

Here $E_{\rm surf}^{\rm sph} = b_{\rm surf}A^{2/3}$, where $b_{\rm surf}$ is the surface tension LD coefficient.
For the neck-radius $r_{\rm neck} = r_0$ and the nucleus radius $R_0 = r_0 A^{1/3}$ one obtains:

$$V_{\rm nuc}(q_{\rm sc}) = -\frac{1}{2}b_{\rm surf} \ , \quad {\rm i.e.,} \quad V_{\rm nuc}(q_{\rm sc}) \approx -9\ {\rm MeV} \ .$$

Light particles evaporation

Thermally excited heavy nuclei deexcite by emitting neutrons, protons, or α-particles.

At relatively low excitation energies ($E^* < 80$ MeV), only neutron evaporation takes place, while the emission of a proton or α-particle is rather unlikely.

Neutron emission width is evaluated according to the Weisskopf theory[a]:

$$\Gamma_{\rm n}(\epsilon_{\rm n}) = \frac{2\mu}{\pi^2\hbar^2\rho_{\rm M}(E^*_{\rm M})} \int_0^{\epsilon_{\rm n}} \sigma_{\rm inv}(\epsilon)\,\epsilon\,\rho_{\rm D}(E^*_{\rm D})\,d\epsilon\ .$$

Here μ is the reduced mass of the neutron, $\sigma_{\rm inv}$ is the neutron inverse cross-section[b]:

$$\sigma_{\rm inv}(\epsilon) = \left[0.76 + 1.93/A^{1/3} + \frac{1.66/A^{2/3} - 0.050}{\epsilon}\right] \pi\,(1.70A^{1/3})^2\ ,$$

while $\rho_{\rm M}$ and $\rho_{\rm D}$ are respectively the level densities of mother and daughter nucleus:

$$\rho(E) = \frac{\sqrt{\pi}}{12a^{1/4}E^{5/4}}\,\exp(2\sqrt{aE})\ ,$$

where $a(q_i)$ is the single-particle level-density parameter (here taken from Ref.[c]).

a) H. Delagrange et al. Z. Phys. A 323, 437 (1986).

b) I. Dostrovsky, Z. Fraenckel, G. Friedlander, Phys. Rev. C 21, 1261 (1980).

c) B. Nerlo-Pomorska, K. Pomorski, J. Bartel, K. Dietrich, Phys. Rev. C 67, 051302 (2002).

Fragment mass yield of spontaneously fissioning ^{252}Cf

The primary fission fragment mass yield obtained in our model is compared with the data*:

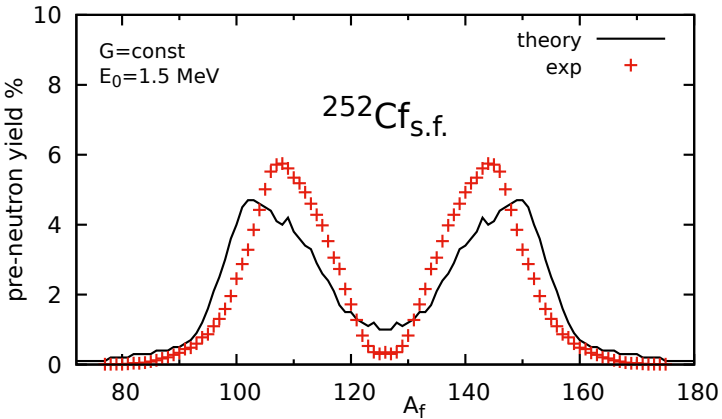

The theoretical yields are shifted by a few mass units concerning the data and probability of the symmetric fission is slightly overestimated.

* A. Al. Adili et al., Nucl Data Seets 107(2006)

TKE of spontaneously fissioning ^{252}Cf

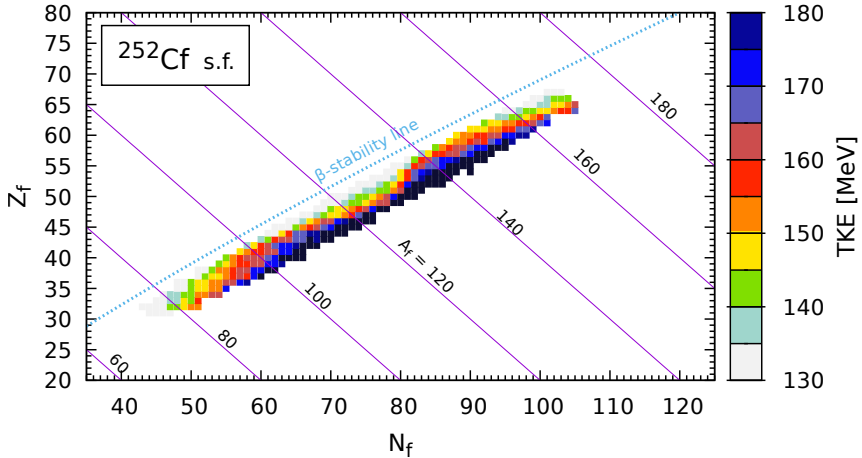

The TKE averag ed over all trajectories, i.e., for each specific fragment pair, is shown as a function of the primary fragment neutron (N_f) and proton (Z_f) numbers. It is seen that the neutron-rich isotopes have, in general, larger TKEs, which means that they correspond to smaller elongations of the fissioning system in the scission configuration.

Multiplicity of neutrons (ν) emitted by ^{252}Cf(sf)

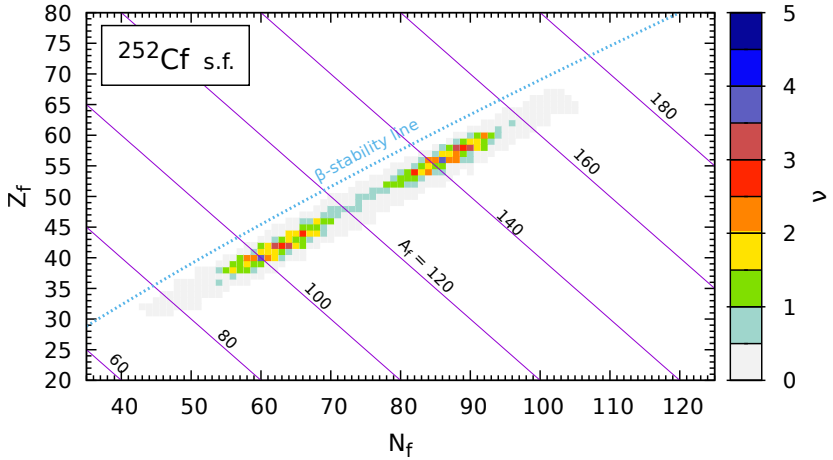

The symmetric fragments emit, on average, less than one neutron, the most probable mass asymmetric fragments evaporate around three neutrons or more. All fission fragments are located below the β-stability line and thus correspond to relatively neutron-rich isotopes, as known for fission.

Isotopic fission fragment yields of ^{252}Cf(sf)

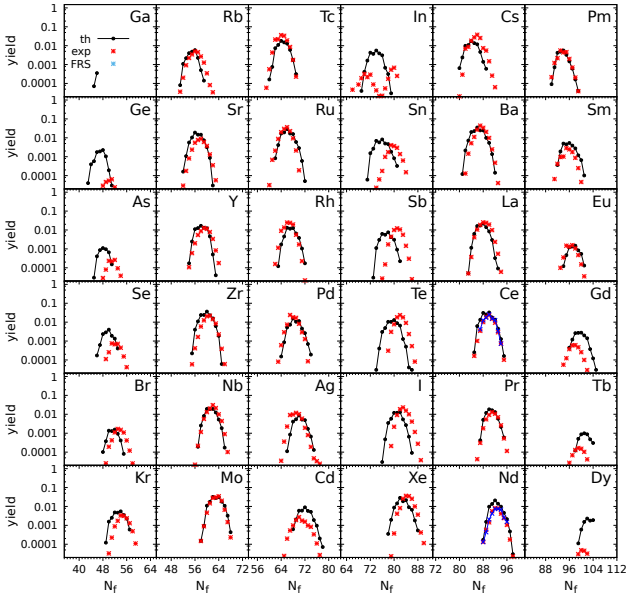

Secondary, i.e., after neutron emission, fission fragment isotopic yields from Ga to Dy. Black points present theoretical estimates, while the experimental data (red stars) are taken from:

M. B. Chadwick et al, Nucl. Data. Sheets **107**, 2931 (2006),

for In isotopes:

A.J.M. Plompen, Eur. Phys. **56**, 181 (2020),

and for Ce and Nd from (blue x):

Y. Waschitz et al,Eur.Phys. J. Web of Conf. **284**, 04005 (2023).

Differential fusion cross-sections for ^{250}Cf production

Langevin code* estimate of the differential fusion cross-section produced in the reaction:

^{238}U + ^{12}C at E_{lab}=1461 MeV

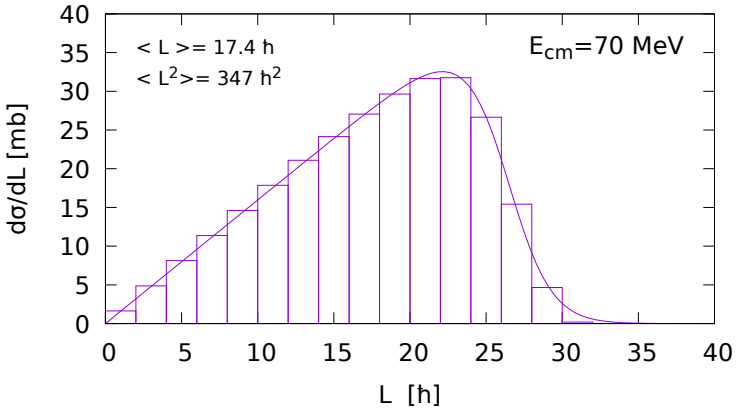

The most probable angular momentum of ^{250}Cf is found to be around $\boldsymbol{L = 20\hbar}$.

* W. Przystupa, K. Pomorski, Nucl. Phys. A 572, 153(1994).

Potential energy surfaces of ^{250}Cf at T=1.4 MeV

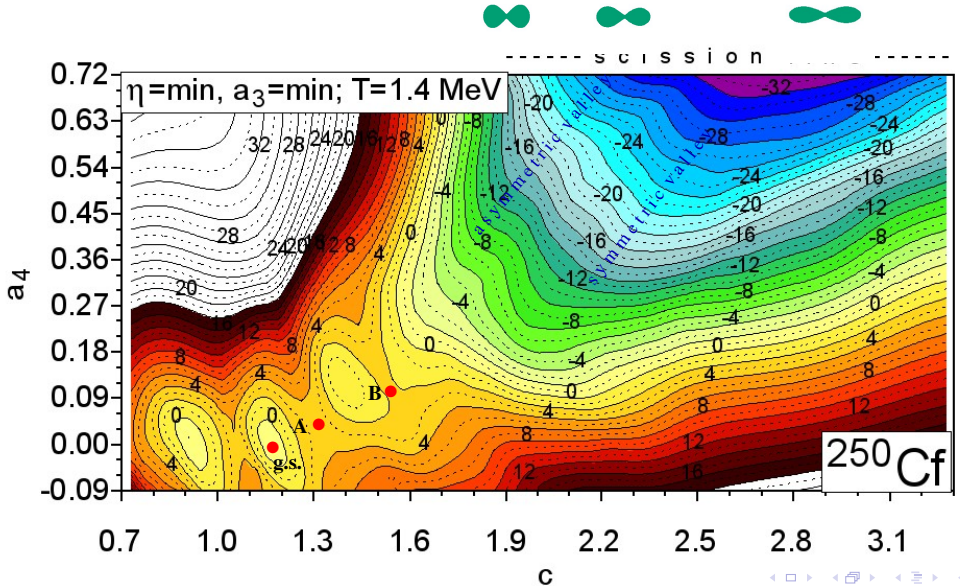

Pre-scission neutron emission probability by excited ^{250}Cf

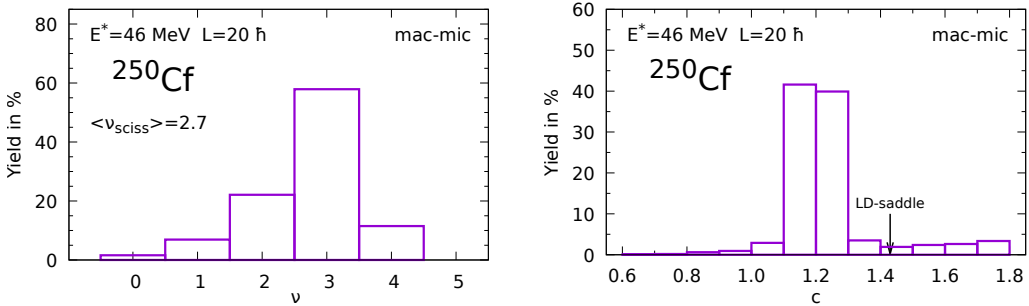

The Langevin+Masters model estimates of the multiplicity of pre-fission neutron emitted by ^{250}Cf at E^*=46 MeV (l.h.s.) and the number of neutrons emitted at a given elongation (c) of fissioning nucleus (r.h.s.).

It is seen that the majority of the pre-fission neutrons are emitted at rather small elongations,i.e., before reaching the saddle point.

Primary fission fragment mass yield of ^{250}Cf at E^*=46 MeV

Due to its relatively high initial excitation energy, the compound nucleus ^{250}Cf produced in a fusion reaction has a high probability of emitting some neutrons before reaching the scission configuration as emission of light-charged particles prior to scission is extremely rare due to the higher energy cost. Particle evaporation before scission leads to what is commonly called multi-chance fission.

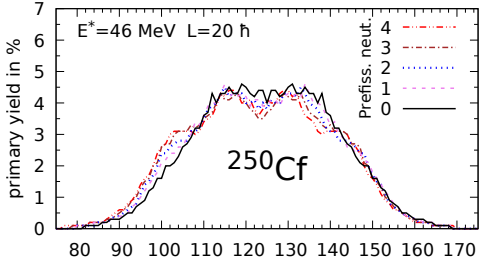

Yields corresponding to the different fission chances.

Distribution probability of the fissioning Cf isotopes obtained after pre-fission neutron emission and their excitation energy:

$\nu_{\mathbf{pre}}$	4	3	2	1	0
Cf	246	247	248	249	250
yield in %	11.5	57.9	22.1	6.9	1.6
$\boldsymbol{E^{\mathrm{th}}}/\mathbf{MeV}$	15.8	20.4	27.3	35.7	45.5

Distribution probability of the fissioning Cf isotopes obtained after pre-fission neutron emission and their excitation energy. $\boldsymbol{E^{\mathrm{th}}}$ refers to the thermal excitation energy, i.e., after subtraction of the rotational energy.

Primary fission fragment TKE yields of ^{250}Cf

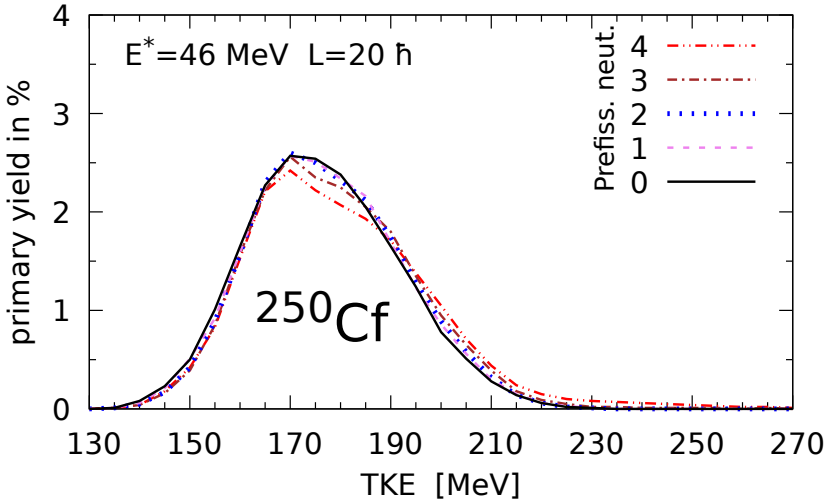

Primary (i.e., at scission configuration) fission fragment TKE yields corresponding to the different fission chances.

Primary and final mass yields of ^{250}Cf

Without prefission neutrons

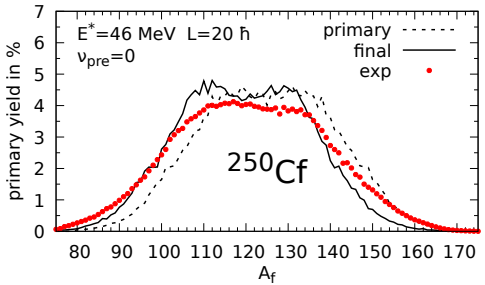

With prefission neutrons

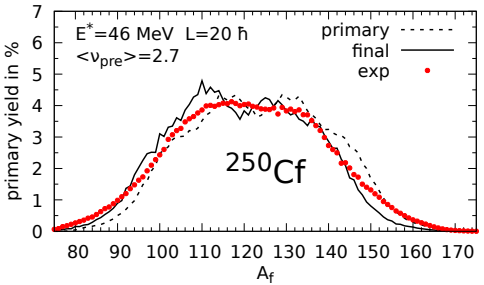

Primary (dashed line) and final (solid line) fission fragment mass yields of ^{250}Cf obtained without (l.h.s.) and with (r.h.s.) considering multi-chance fission.

The experimental data (red diamonds) are taken from:

D. Ramos et al, Phys. Rev. 99, 024615 (2021).

Charge yields of ^{250}Cf

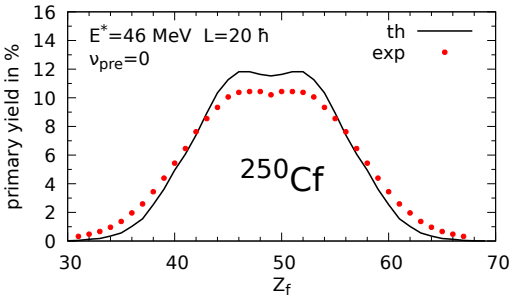

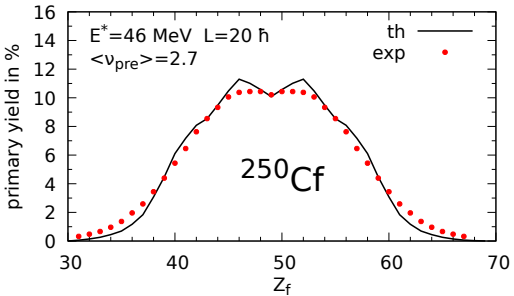

Final (solid line) fission fragment charge yields of ^{250}Cf obtained without (r.h.s.) and with (l.h.s.) considering multi-chance fission.
The experimental data (red diamonds) are taken from: D. Ramos et al, Phys. Rev. 99, 024615 (2021).

The estimates obtained by taking into account the pre-fission neutron evaporation, evaluated separately for different Cf isotopes and then weighted, are closer to the data.

Experimental and theoretical isotopic yields of ^{250}Cf

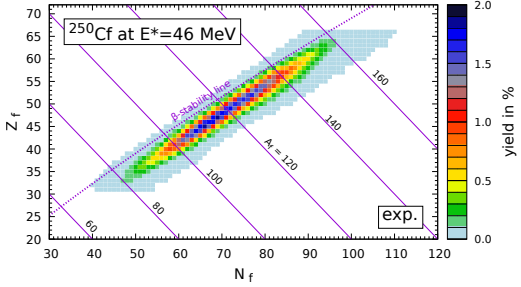

Experimental isotopic yields of ^{250}Cf.

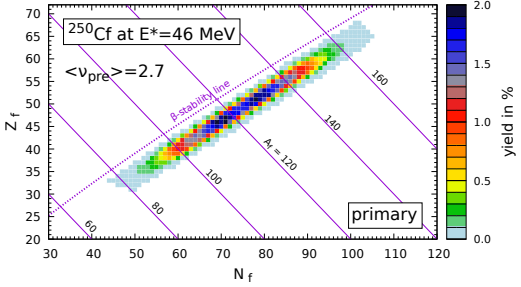

Primary isotopic yields.

The calculations are based on $\mathbf{5 \times 100\,000}$ Langevin trajectories.

The experimental data are taken from: D. Ramos et al, Phys. Rev. **99**, 024615 (2021).

Final isotopic yields of ^{250}Cf

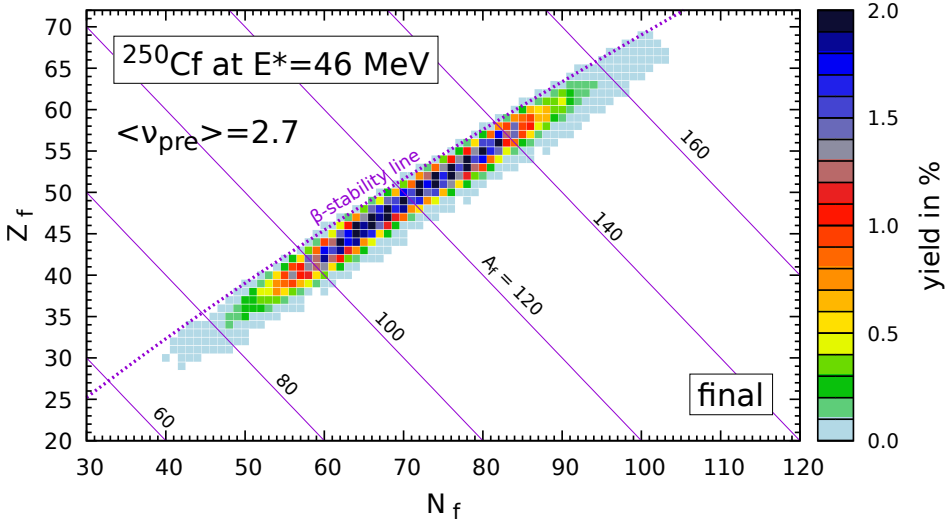

The final distribution of yields, i.e., after neutron emission from the fragment, is found to be shifted by 2-3 units relative to the measured ones.

Total kinetic energy yields for primary fragments

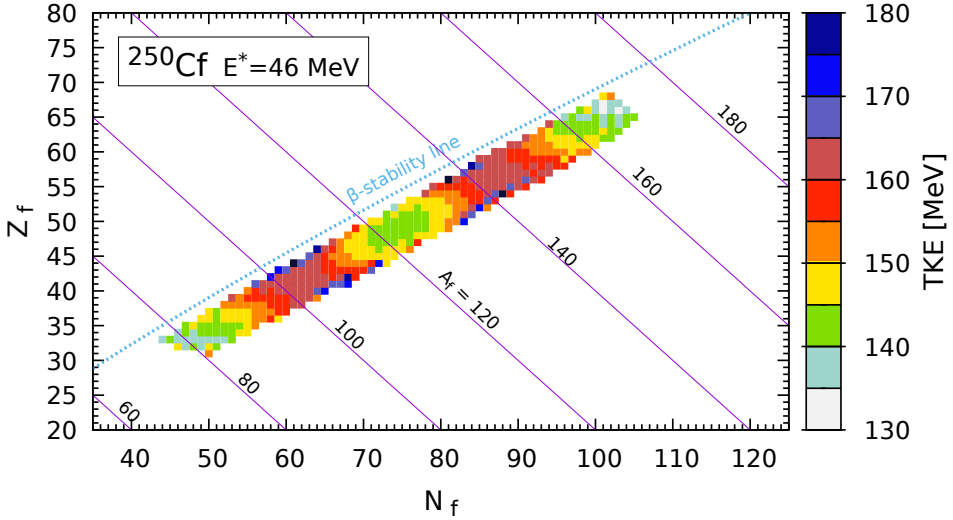

Our model predicts a small TKE around 140 MeV for the symmetic fission, while the fragments with masses around $\boldsymbol{A = 140}$ or $\boldsymbol{A = 110}$ have larger TKE's around 160 MeV.

Secondary fragment isotopic yields for Ga to Dy

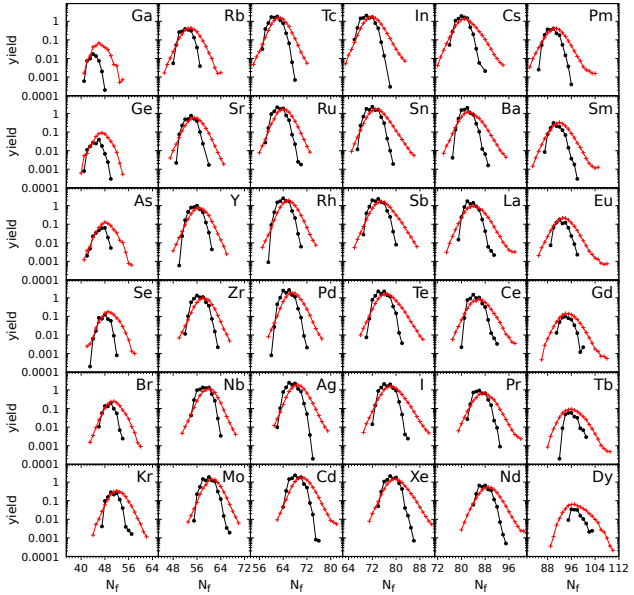

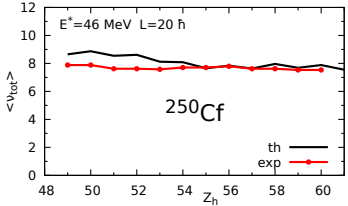

Total neutron multiplicity as a function of fragment charge number.

⟵ The fragment isotopic yields of ^{250}Cf at E* 46 MeV. Theoretical estimates (•) are compared with the experimental data (+) taken from:

D. Ramos et al, Phys. Rev. 99, 024615 (2021)

Summary:

- Fourier over Spheroid expansion offers a very effective way of describing the shapes of fissioning nuclei both in vicinity of the ground-state and the scission point.
- The macroscopic LSD energy with the shell and pairing microscopic corrections was used to determine the potential energy surfaces in the 4D (c, a_3, a_4, η) space.
- Multi-dimensional 3D $(c, a_3, a_4; \eta_{\min})$ Langevin fission model is capable of handling the various facets of the process, including:
  (a) dynamical evolution of the fissioning system between the ground state and the scission point in competition with the particle evaporation,
  (b) sharing of neutrons, protons, and excitation energy between the two fragments at the moment of scission,
  (c) fission fragment primary and secondary mass, charge and TKE yields,
  (d) decay of compound nucleus to evaporation residues through the emission of neutrons.

Thank you for your attention!

Random Langevin force

The vector $\vec{F}(t)$ stands for the random Langevin force, which couples the collective dynamics to the intrinsic degrees of freedom and is defined as:

$$F_i(t) = \sum_j g_{ij}(\vec{q})\ G_j(t)\ ,$$

where $\vec{G}(t)$ is a stochastic function whose strength $g(\vec{q})$ is given by the diffusion tensor $\mathcal{D}(\vec{q})$ defined by the red generalized Einstein relation:

$$\mathcal{D}_{ij} = T^* \gamma_{ij} = \sum_k g_{ik}\ g_{jk}\ ,$$

with effective temperature*

$$T^* = E_0 / \tanh\left(\frac{E_0}{T}\right)\ ,$$

which takes into account both statistical and collective fluctuations. In the following, we have taken $E_0 = 3 \times 0.5$ MeV, assuming that each collective mode contributes 0.5 MeV to the zero-point energy.

*K. Pomorski, H. Hofmann, J. Physique 42, 381 (1981).

Temperature of fissioning nucleus

The temperature T is obtained from the thermal excitation energy of nucleus E^* defined as the difference between the initial energy E_{init} and the final one, which is the sum of kinetic (E_{kin}) and potential energies o f nucleus at the actual deformation point ($\vec{q}$) and the sum of the binding and the kinetic energies of emitted particles (E_{part}):

$$a(\vec{q})T^2 = E^*(\vec{q}) = E_{\mathrm{init}} - [E_{\mathrm{kin}}(\vec{q}) + E_{\mathrm{pot}}(\vec{q}, 0) + E_{\mathrm{part}}] \,,$$

where $a(\vec{q})$ is the single-particle level density.
For every single trajectory, we evaluate T after every 200 steps when solving the Langevin equation as long as the system reaches the scission point, i.e., when the neck radius will be equal to the nucleon radius $r_{\mathrm{neck}} = r_0 = 1.217$ fm, what happens when $a_4 \approx 0.72$.
Above procedure allows to conserve approximately the total energy of the fissioning system, which is truncated in each Langevin step due to the effect of the random force*

*H. J. Krappe and K. Pomorski, *Theory of Nuclear Fission*, Series: Lecture Notes in Physics, Vol. 838, Springer Verlag, 2012.

Details of the calculation

Our calculation is performed in the 4D FoS deformation parameters space:

$$\eta \in [0, 0.21],\ c \in [0.6, 3.3],\ a_3 \in [0, 0.51],\ a_4 \in [-0.09, 0.72]$$

The non-axial deformation η was found to be significant only at small elongations (c) before reaching the outer saddle ($c \approx 1.6$). The role of higher-order Fourier expansion coefficients a_5 and a_6 is small even in the region of well-separated fission fragments.

So, we have restricted the Langevin calculations to the 3D (c, a_3, a_4) space when discussing fission dynamics. The non-axial deformation η is included only in a static way by minimization of the E_{pot} with respect to the non-axial degree of freedom.

Using the above formalism and procedure, we have performed extended dynamical calculations, including up to $5 \cdot 10^5$ Langevin trajectories, from which we extracted the predictions of the model for various observables such as the fission fragment masses, charge, or kinetic energy distributions.

In our calculation, we have assumed that the masses of the heavy (A_{h}, $\vec{q}_{\mathrm{h}}$) and the light fragments (A_l, $\vec{q}_l$) are proportional to the volumes of the daughter nuclei at the scission point.

The fragments N_f/Z_f and neutron multiplicities

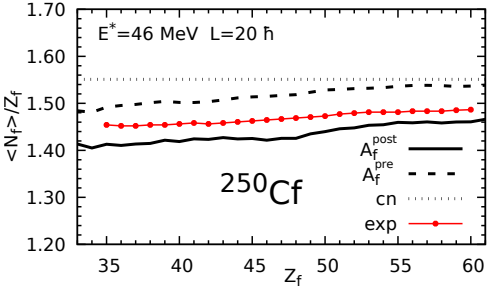

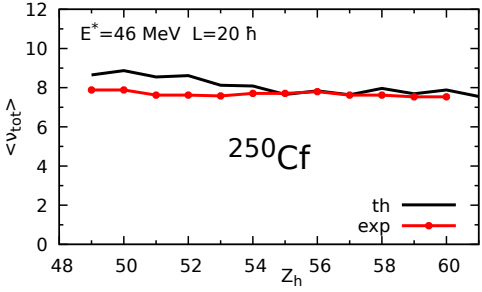

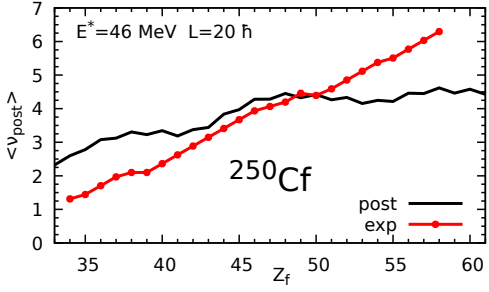

The average fragment N_f/Z_f ratio as function of the fragment charge number (top, l.h.s.). The total (top, r.h.s.) and the post-fission neutron numbers (bottom) per fragment as function of the heavy fragment charge number of ^{250}Cf at $E^* = 46$ MeV. The experimental data (red) are taken from:

D. Ramos et al, Phys. Rev. 99, 024615 (2021).